

Physicochemical Characterization and Corrosion Inhibition Potential of *Ficus benjamina* (FB) Gum for Aluminum in 0.1 M HCl

Nnabuk Okon EDDY^{1,*}, Paul Ocheje AMEH² and Ali IBRAHIM¹

¹Department of Chemistry, Ahmadu Bello University, Zaria Kaduna State, Nigeria

²Physical Chemistry Unit, Department of Chemistry, Nigeria Police Academy, Kano State Nigeria

(*Corresponding author's e-mail: nabukeddy@yahoo.com, nocaseoche@yahoo.com)

Received: 30 July 2014, Revised: 1 September 2014, Accepted: 17 September 2014

Abstract

Examination of the physical (colour, odour, pH, solubility in various solvent) and chemical (GCMS and FTIR) characteristics of *Ficus benjamina* gum revealed that the gum is yellowish in colour, mildly acidic and ionic in nature. Major constituents of the gums were found to be sucrose and d-glucose, which constituted 60.92 % of its chemical constituents while various carboxylic acids (albiatic acid (1.00 %); hexadecanoic acid (4.41 %); 9-octadecanoic acid (1.00 %), stearic acid (3.01 %); oleic acid (0.10 %); octadecanoic acid (9.12 %) and 6,13-pentacenequinone (20.43 %) accounted for the remaining constituents. Functional groups identified in the gum were found to be those typical for other carbohydrates. From the knowledge of the chemical structures of compounds that constitutes the gum, the corrosion inhibition potentials of the gum was ascertained and from weight loss analysis, the gum was found to be an active inhibitor against the corrosion of aluminum in solutions of tetraoxosulphate (VI) acid. The gum acted as an adsorption inhibitor that favours the mechanism of chemical adsorption and supported the Frumkin and Dubinin-Radushkevich adsorption models.

Keywords: *Ficus benjamina* gum, physicochemical characteristics and corrosion inhibition

Introduction

Industrial revolution over the past centuries has provoked an increase in the use of metals and their alloys for the fabrication of several installations. Some processes (such as acid wash, pickling and etching) within the oil, fertilizer, metallurgical and other industries expose metallic components to corrosion [1]. In view of this, several steps have been taken to protect metals against corrosion but one of the best options involves the use of inhibitors [2,3]. Inhibitors are substances which when present in minute quantities is able to retard the corrosion of the metal through the mechanism of adsorption [4].

Most of the suitable and documented corrosion inhibitors for metals are heterocyclic compounds such as carbozones, quinolones, amines, amino acids, carbohydrates, polymers, plant extracts, chromates, etc [5-11]. Of significant interest is the use of plant and animal extracts because they are natural, less toxic, biodegradable and easily accessible compared to those that are not ecofriendly [12].

The use of plant products as corrosion inhibitors is justified by the phytochemical components of the plant, some of which have chemical structures that meet the requirements needed for corrosion inhibition [13]. Exudate gums from plants have proven to be viable as corrosion inhibitors because they offer large adsorption sites, they are biodegradable, less toxic and can easily be gotten from gum bearing plants. Some of the gums that have been found to be good corrosion inhibitors include *Khaya ivorensis* gum exudate [14], *Daniella Oliverri* gum [15], Guar gum [16], *Commiphora pedunculata* gum [17], *Ferula assa-foetida* and *Dorema ammoniacum* gum exudates [18], *Acacia seyal* var. [12], *Ficus tricopoda* [19] and *Raphia hookeri* gum [11]. Literature is however scant on the use of *Ficus benjamina*

(*FB*) gum as a corrosion inhibitor. Therefore, the present study is aimed at carrying out physicochemical, GCMS and FTIR analysis of *FB* gum and to investigate the corrosion inhibition potential of the gum.

Materials and methods

A sample of *FB* gum was tapped from the *Ficus* species of the plant in Kanya Babba village, located in Babura Local Government area of Jigawa state, Nigeria. A crude sample of the gum was purified using the method described by Eddy *et al.* [19].

Physicochemical analysis

The pH of the gum was determined using a pre-calibrated Oklon pH meter. The solubility of the gum was determined in cooled and hot distilled water, acetone and chloroform using the method reported by Carter [20].

FTIR analysis

FTIR analysis of the gum and that of the corrosion products (in the absence and presence of gum) were carried out using Shimadzu FTIR-8400S Fourier transform infra-red spectrophotometer. The sample was prepared in KBr and the analysis was carried out by scanning the sample from 400 to 4000 cm^{-1} .

GC-MS analysis

GC-MS analysis was carried out as described by Eddy *et al.* [21]. Interpretation of the mass spectrum GC-MS was conducted using the database of the National Institute Standard and Technology (NIST) Abuja, having more than 62,000 patterns. The spectrum of the unknown component was compared with the spectrum of the known components stored in the NIST library. The name, molecular weight and structure of the components of the test materials were ascertained. The concentrations of the identified compounds were determined through area and height normalization.

Corrosion studies

Aluminum alloy sheets of composition (wt. %, as determined by quantimetric method) Mn (1.28 %), Pb (0.064 %), Zn (0.006 %), Ti (0.029 %), Cu (0.81 %), Si (0.381 %), Fe (0.57 %) and Al (96.65 %) were used for the study. The sheet was mechanically pressed cut into different coupons, each $5 \times 4 \times 0.11$ cm in size. Each coupon was degreased by washing with ethanol, cleaned with acetone and allowed to dry in the air before preservation in a desiccator. All reagents used for the study were reagent grade and double distilled water was used for their preparation.

Weight loss experiments were carried out as reported elsewhere [17]. From weight loss measurements, inhibition efficiency (%*I*), corrosion rate (*CR*) and degree of surface (θ) coverage were calculated using the following equations;

$$\%I = \left(1 - \frac{W_1}{W_2}\right) \times 100 \quad (1)$$

$$\theta = \left(1 - \frac{W_1}{W_2}\right) \quad (2)$$

$$CR = \frac{\Delta W}{At} \quad (3)$$

where W_1 and W_2 are the weight losses (g) for aluminum in the presence and absence of the inhibitor, θ is the degree of surface coverage of the inhibitor, $\Delta W = W_2 - W_1$, A is the area of the aluminum coupon (in cm^2), t is the period of immersion (in hours) and ΔW is the weight loss of aluminum after time, t .

Results and discussion

Physicochemical parameters of *FB* gum

Physicochemical parameters of *FB* gum are presented in **Table 1**. From the results obtained, it was found that *FB* gum is yellowish in color (**Figure 1**). It has a sweet taste and exhibited an odour similar to that of cocoa.

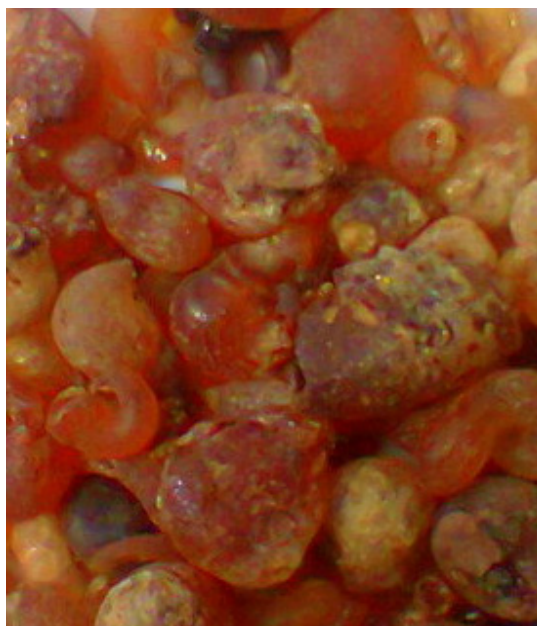


Figure 1 Photographs of crude sample of *FB* gum.

Table 1 Physicochemical properties of *FB* gum.

Parameter	
Colour	Yellow
Odour	Cocoa smell
Taste	Sweet
pH (28 °C)	5.5
Percentage yield (%w/w)	58
Solubility (%w/v)	
Cold water	11.2
Hot water	10.2
Acetone	0.8
Chloroform	0.00
Ethanol	1.0

The gum is mildly acidic with a pH of 5.5. After purification, a gum yield of 55 % was obtained. *FB* gum is ionic, soluble in cold and hot water. The solubility of the gum was found to decrease with an increase in temperature. The gum is sparingly soluble in acetone and ethanol but insoluble in chloroform.

GC-MS and FTIR studies

The GCMS spectrum of the *FB* gum is presented in **Figure 2** while **Table 2** presents information deduced from the spectrum. Names of identified compounds, chemical formula, molar mass and concentrations (determined through area normalization) are also presented in **Table 2** while the chemical structures of these compounds are presented in **Figure 3**. The spectrum revealed nine peaks, identified between the retention time of 25.56 to 33.21 min. The identified compounds included, albiotic acid (1.00 %), hexadecanoic acid (4.41 %), 9-octadecanoic acid (1.00 %), stearic acid (3.01 %), oleic acid (0.10 %), octadecanoic acid (9.12 %), 6,13-pentacenequinone (20.43 %), d-glucose (18.69 %) and sucrose (42.23 %). From the above results, it can be seen that the dominant component of *FB* gum is carbohydrate (i.e sucrose and d-glucose), constituting 60.92 % of the entire sample. Other samples were carboxylic acids indicating that, like other exudate gum, *FB* gum is rich in polysaccharides and carboxylic acids.

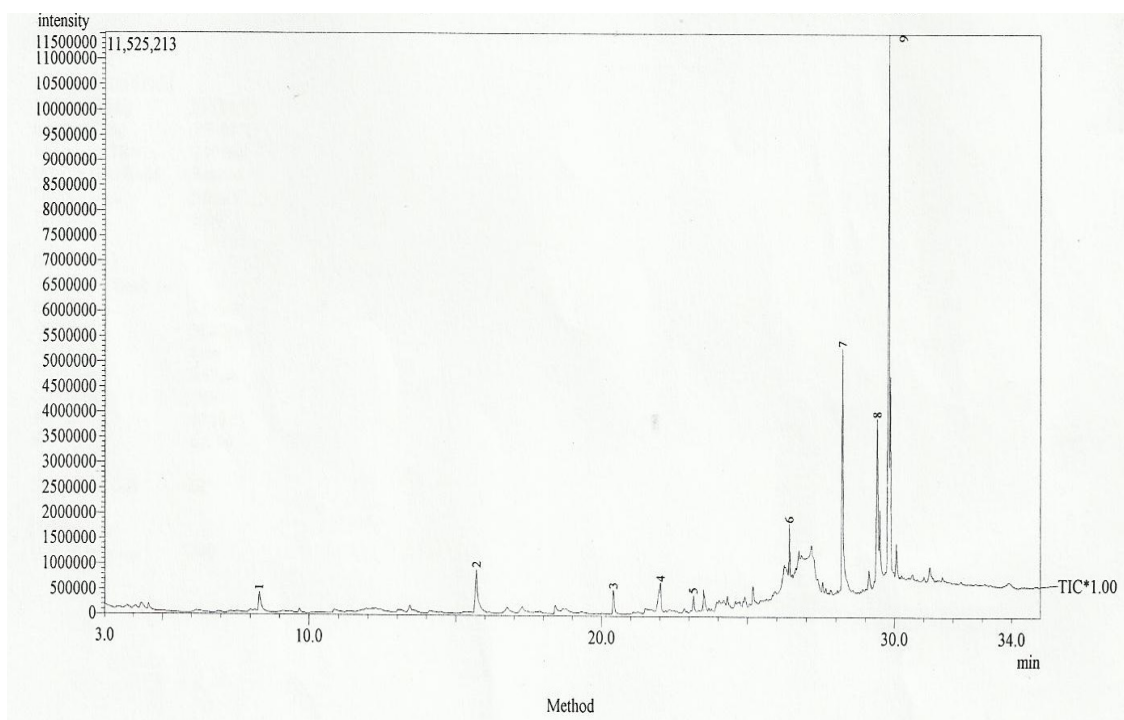


Figure 2 GC-MS spectrum of *FB* gum.

Table 2 Characteristics of compounds identified in the GC-MS of *FB* gum.

Line no	IUPAC Name	Molecular formula	Molar mass (g/mol)	RT (minutes)	Mass peak	% Conc.
1	Albeitic acid	C ₂₀ H ₃₀ O ₂	302	33.216	78	1.00
2	n-hexadecanoic acid	C ₁₆ H ₃₂ O ₂	256	30.525	84	4.41
3	9-Octadecanoic acid	C ₁₈ H ₃₄ O ₂	282	29.004	92	1.00
4	Stearic acid	C ₁₈ H ₃₆ O ₂	284	31.157	86	3.01
5	Oleic acid	C ₁₈ H ₃₄ O ₂	282	27.117	83	0.11
6	Octadecanoic acid	C ₁₈ H ₃₆ O ₂	284	27.258	66	9.12
7	6,13-pentacenequinone	C ₂₂ H ₁₂ O ₂	308	25.555	52	20.43
8	d-glucose	C ₁₂ H ₂₄ O ₁₂	360	30.558	96	18.69
9	Sucrose	C ₁₂ H ₂₂ O ₁₁	342	32.914	78	42.23

Figure 4 presents the FTIR spectrum of *FB* gum. Peaks and frequencies of adsorption deduced from the spectrum as well as assigned bonds/functional groups are recorded in **Table 3**. From the results obtained, it is evident that several stretches and vibrations, typical for polysaccharides are found in the FTIR spectrum of *FB* gum. These included OH stretches and vibrations due to carboxylic acids at 2727 and 2764, 2990, 3308 and 3469 cm⁻¹, OH stretch due to alcohol or phenol was found at 3160 cm⁻¹, C-H stretch due to alkane at 2868 cm⁻¹, C-H scissoring and bending vibrations at 1356 cm⁻¹, C=O stretch due to aldehyde, ketone, ester and carboxylic acid at 1716 cm⁻¹, O-H stretch at 3308 and 3469 cm⁻¹, C-O vibration due to carboxylic acid and alcohol at 1005 cm⁻¹. The presence of an aromatic ring at 1602 cm⁻¹ was also observed.

Table 3 Peaks and intensity of IR adsorption by *FB* gum.

Peak	Intensity	Area	Assignments/functional groups
705	40.054	35.038	C-H bend
796	35.551	54.017	C-H bend due to alkene
1005	29.927	130.096	C-O stretch due to carboxylic acid, ether, alcohol or esters
1157	30.663	38.450	C-O stretch due to carboxylic acid, ether, alcohol or esters
1277	27.593	82.798	NO ₂ symmetric stretch due to nitro compound
1356	28.072	94.912	C-H scissoring and bending vibrations
1602	26.747	75.593	Aromatic ring
1716	30.734	72.856	C=O stretch due to aldehyde, ketone, carboxylic acid and ester
2154	47.310	109.327	C≡C stretch due to alkyne
2727	29.512	191.569	OH stretch due to carboxylic acid
2764	29.512	33.671	OH stretch due to carboxylic acid
2868	28.699	64.702	C-H stretch due to alkane
2990	28.958	71.045	OH stretch due to carboxylic acid
3160	27.980	91.055	OH stretch due to phenol and alcohol
3308	30.104	93.474	OH stretch due to carboxylic acid
3469	33.943	38.317	OH stretch due to carboxylic acid
3554	34.052	98.462	OH stretch due to hydrogen bond in alcohol or phenol

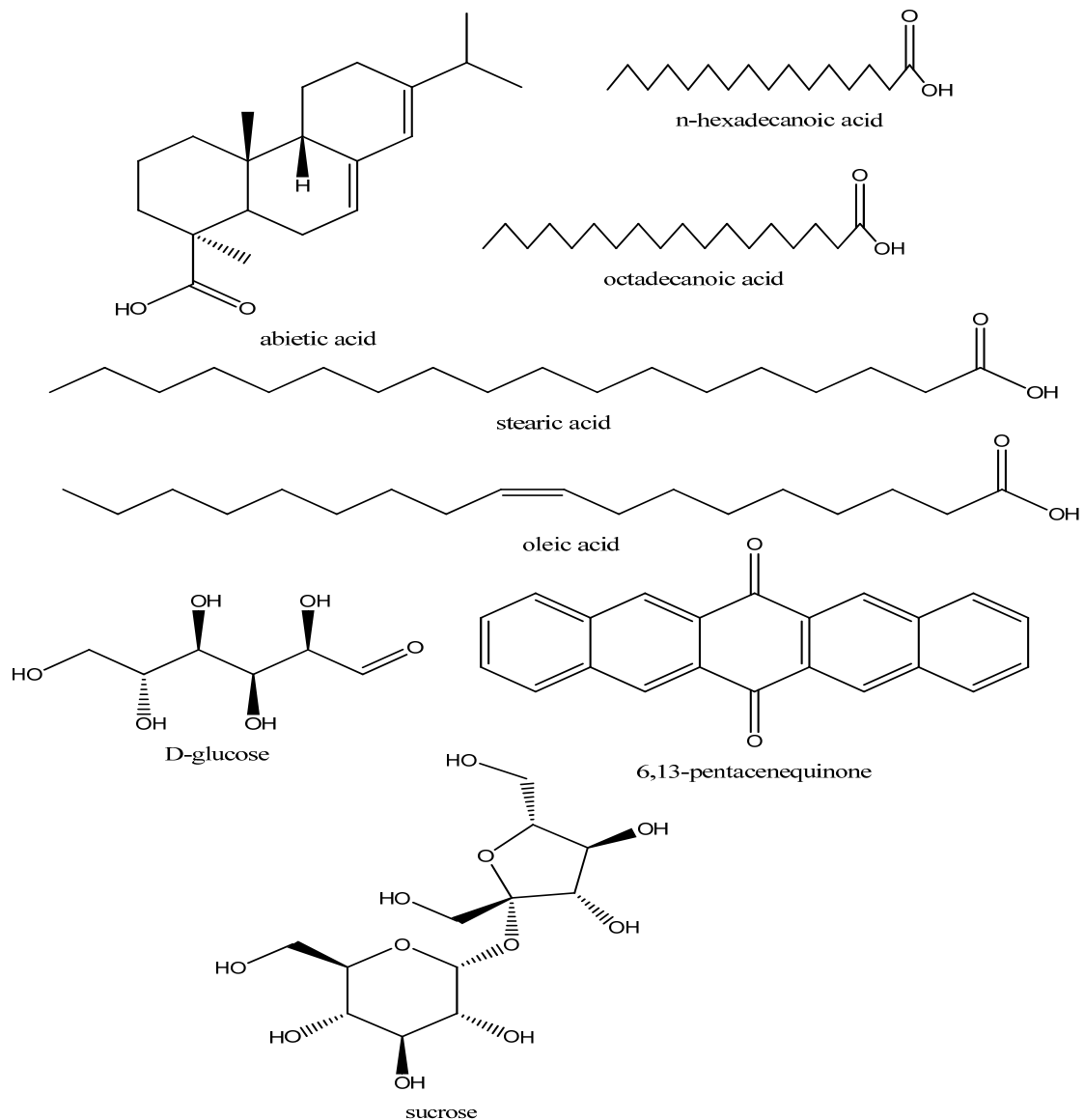


Figure 3 Chemical structures of the compounds in *FB* gum.

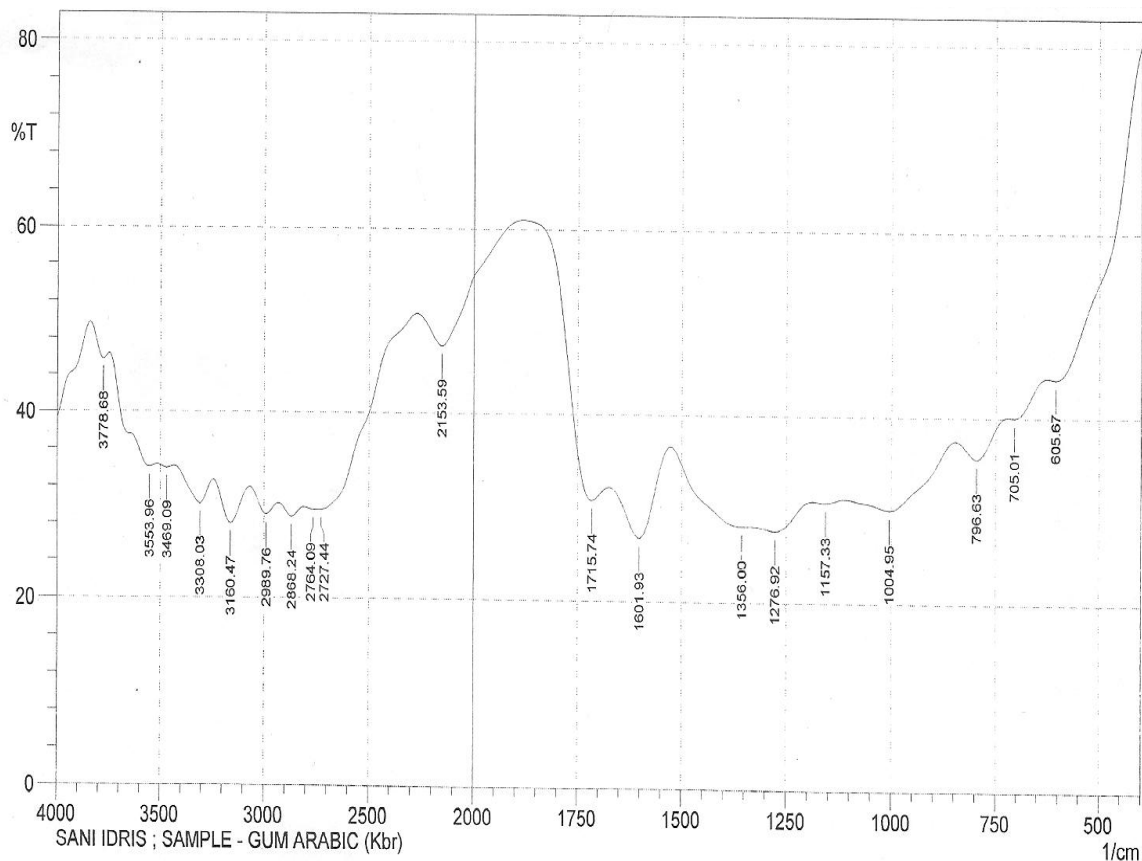


Figure 4 FTIR spectrum of *FB* gum.

Corrosion inhibition study

Effect of *Ficus benjamina* gum on the corrosion of Al

Figure 5 shows the variation in weight loss with time for the corrosion of Al in a solution of HCl containing various concentrations of *FB* gum at 303 and 333 K, respectively. It is evident from the figures that weight loss of mild steel increases with an increase in the period of contact but decreases with an increase in the concentration of the *FB* gum. These observations indicated that *FB* gum inhibited the corrosion of mild steel by reducing its rate of corrosion and that the inhibition efficiency of *FB* gum increases with an increase in its concentration. Therefore, *FB* gum is an adsorption inhibitor, characterized by an increase in inhibition efficiency with concentration [22]. It was also found that the corrosion rate of Al in the presence of the inhibitor (Table 4) decreases with an increase in temperature while its inhibition efficiency increases with an increase in temperature indicating that the adsorption of *FB* gum on the surface of Al supports the mechanism of chemical adsorption. Chemisorption is characterized by an increase in the extent of adsorption with temperature as opposed to physisorption, which compromises a decrease in the extent of adsorption with temperature [5].

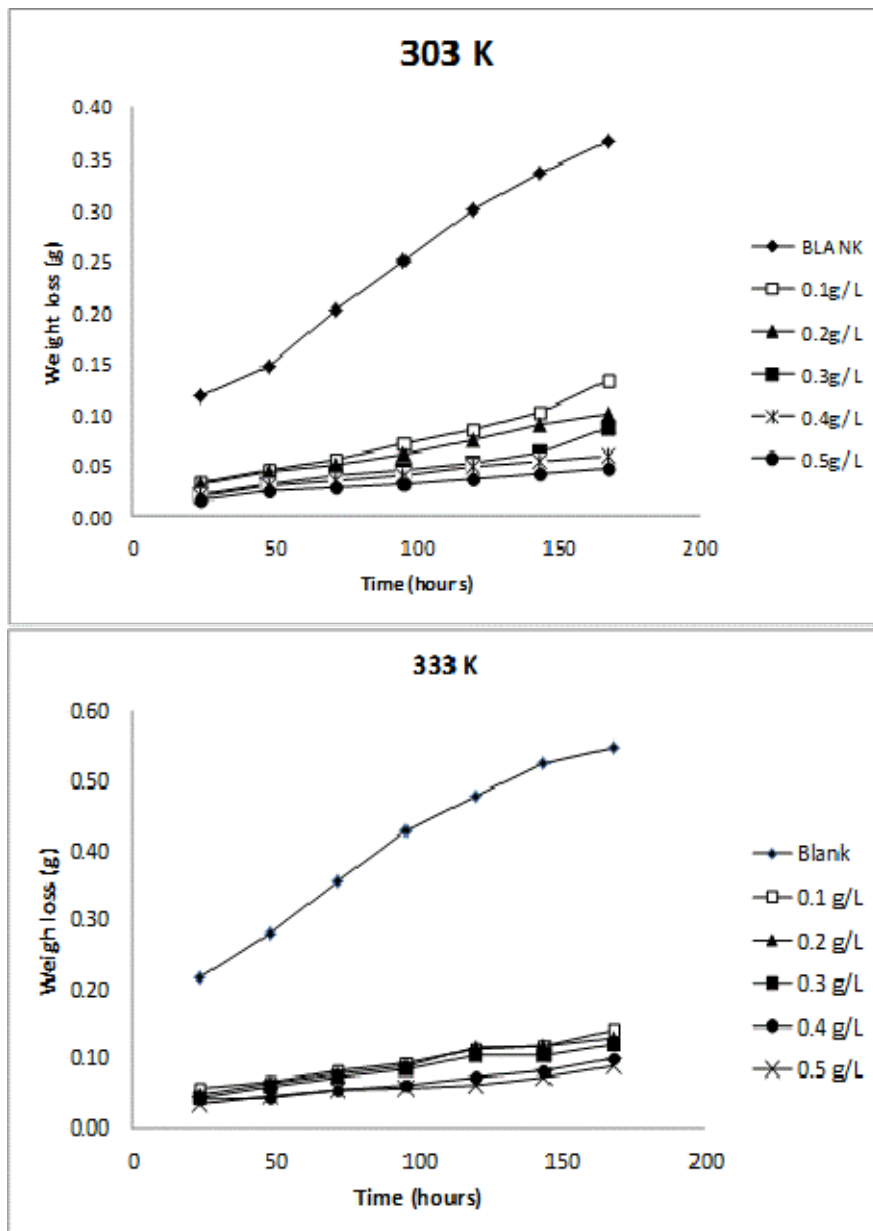


Figure 5 Variation of weight loss with time for the corrosion of Al in HCl containing various concentrations of *FB* gum at 303 and 333 K.

Table 4 Corrosion rates for Al, inhibition efficiency and degree of surface coverage of *FB* gum in 0.1 M HCl.

C (g/L)	CR (g/cm ³ /h) at 303 K	% I (303 K)	θ (303 K)	CR (g/cm ³ /h) at 333 K	% I (333 K)	θ (333 K)
Blank	1.09×10 ⁻⁴	-	-	16.3×10 ⁻⁴	-	-
0.1	3.93×10 ⁻⁵	64.00	0.640	4.19×10 ⁻⁴	74.29	0.743
0.2	2.98×10 ⁻⁵	72.80	0.728	3.83×10 ⁻⁴	76.50	0.765
0.3	2.53×10 ⁻⁵	76.80	0.768	3.57×10 ⁻⁴	78.10	0.781
0.4	1.76×10 ⁻⁵	82.52	0.825	2.95×10 ⁻⁴	83.90	0.839
0.5	1.37×10 ⁻⁵	83.74	0.837	2.65×10 ⁻⁴	87.50	0.875

Kinetic study

It has been found that most corrosion reactions are first order indicating that it follows a model, that can be represented as follows [15];

$$-\log(\text{weight loss}) = \frac{k_1 t}{2.303} \quad (4)$$

where *t* is the period of contact and *k*₁ is the first order rate constant. Also, for a first order reaction, the half-life (*t*_{1/2}) is related to the rate constant thus, *t*_{1/2} = 0.693/*k*₁. **Figure 6** shows plots for the variation of -log (weight loss) with time for the corrosion of Al in the absence and presence of *FB* gum as an inhibitor (at 303 and 333 K). The plots revealed excellent correlation (*R*² ≈ 1) indicating the application of Eq. (4) to the corrosion of Al (in the absence and presence of *FG* gum). Values of *k*₁ and *t*_{1/2} deduced from the slope of the plots are presented in **Table 5**. The half-lives for solutions containing various concentrations of *FB* gum are higher than that of the blank and were found to increase with increasing concentration. Therefore, *FG* gum is a good inhibitor for the corrosion of Al.

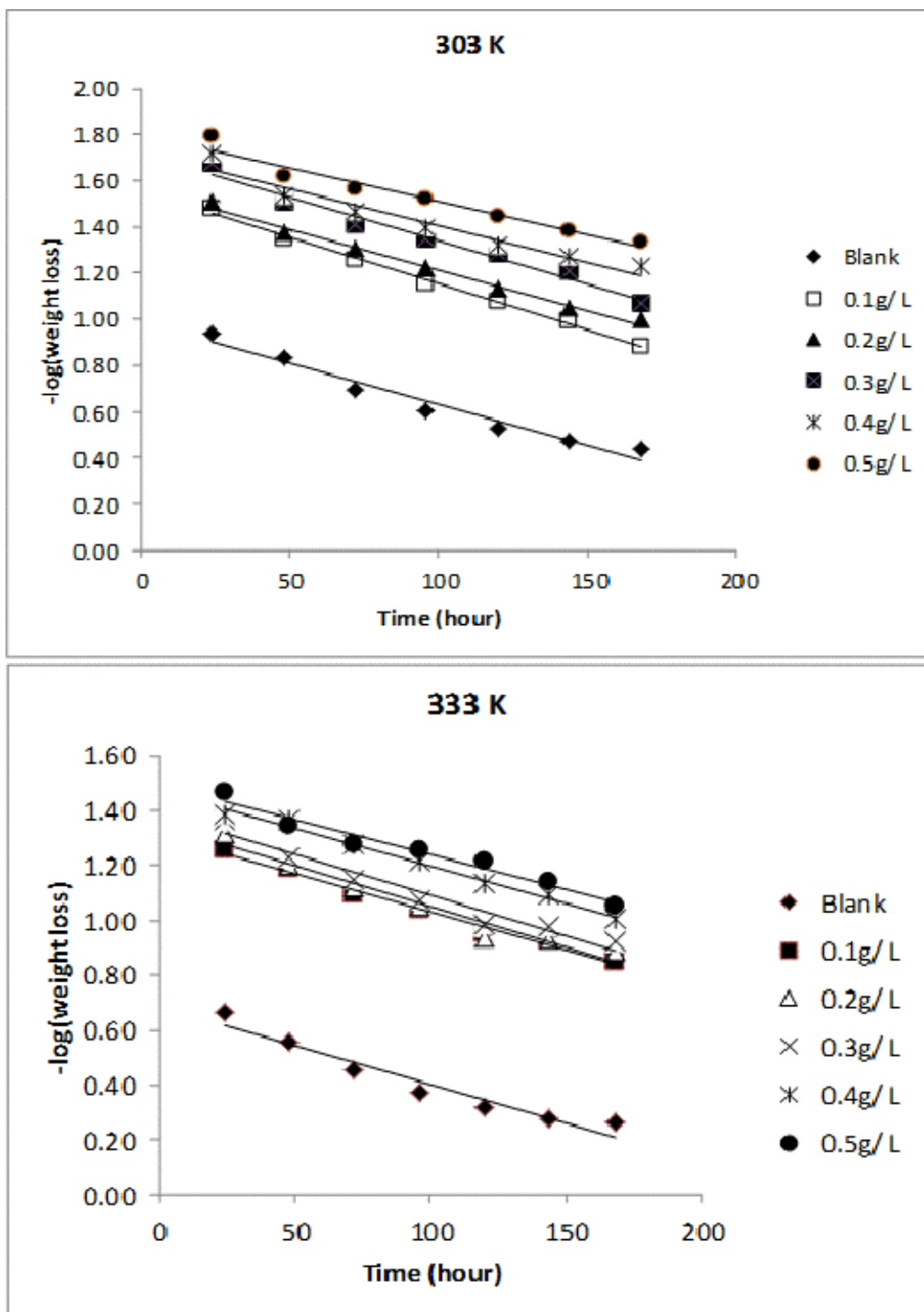


Figure 6 Variation of $-\log(\text{weight loss})$ with time for the corrosion of Al in 0.1 M HCl containing various concentrations of *FB* gum at 303 and 333 K.

Table 5 Kinetic parameters for the corrosion of Al in 0.1 M HCl containing various concentrations of *FB* gum.

T (K)	C (g/L)	Slope	Intercept	k ₁	R ²	t _{1/2} (hour)
303 K	Blank	0.0036	0.9860	0.0083	0.9634	70
	0.1	0.0040	1.5551	0.0092	0.9947	84
	0.2	0.0035	1.5651	0.0081	0.9897	86
	0.3	0.0038	1.7218	0.0088	0.9732	89
	0.4	0.0032	1.7284	0.0074	0.9437	94
	0.5	0.0029	1.8059	0.0067	0.9512	104
333 K	Blank	0.0028	0.6843	0.0064	0.9377	100
	0.1	0.0028	1.3128	0.0064	0.9860	107
	0.2	0.0030	1.3508	0.0069	0.9558	107
	0.3	0.0030	1.3866	0.0069	0.9505	107
	0.4	0.0027	1.4735	0.0062	0.9890	111
	0.5	0.0026	1.4974	0.0060	0.9605	116

Effect of temperature

Activation energies for the corrosion of aluminum in the absence and in the presence of *FB* gum were estimated using the logarithm form of the Arrhenius equation, which can be expressed as follows [14];

$$\log \frac{CR_2}{CR_1} = \frac{E_a}{2.303R} \left(\frac{1}{T_1} - \frac{1}{T_2} \right) \tag{5}$$

where CR₁ and CR₂ are the corrosion rates of mild steel at the temperatures, T₁ (303 K) and T₂ (333 K) respectively, E_a is the activation energy and R is the gas constant. Values of E_a calculated from Eq. (5) are recorded in **Table 5**. From the results obtained, values of E_a ranged from 66.26 to 82.94 kJ/mol and are relatively comparable to the threshold value (80 kJ/mol) expected for the mechanism of chemical adsorption. Generally, lower values of E_a indicate a tendency towards physisorption while higher values of E_a points towards chemisorption. The present results suggest that the adsorption of *FG* gum on the surface of Al must have first proceeded through the mechanism of physical adsorption and was succeeded by chemisorption.

Thermodynamic/adsorption considerations

The heat of adsorption of *FB* gum on the Al surface was calculated using the following equation [15];

$$Q_{ads} = 2.303R \left(\frac{\theta_2}{1 - \theta_2} - \frac{\theta_1}{1 - \theta_1} \right) \times \left(\frac{T_1 \times T_2}{T_2 - T_1} \right) \tag{6}$$

where R is the universal gas constant, θ₂ and θ₁ are the degree of surface coverage at the temperatures T₁ (303 K) and T₂ (333 K), respectively. Calculated values of Q_{ads} for various concentrations of *FB* gum are

also presented in **Table 5**. The adsorption enthalpies are positive for all concentrations of *FB* gum indicating that the adsorption of *FB* gum on the surface of Al is endothermic.

Adsorption isotherms are useful in studying the adsorption characteristics of corrosion inhibitors and was established by fitting data obtained for degree of surface coverage into various adsorption models including the Langmuir, Frumkin, Hill de-Boer, Parsons, Temkin, Flory-Huggin, Freundlich, Dhar-Flory-Huggin, kinetic/thermodynamic model of El-Awady *et al.* and BockrisSwinkels. The general form of an equation representing adsorption isotherms can be written as follows [23];

$$f(\theta, x) \exp(-2a\theta) = bC \quad (7)$$

where $f(\theta, x)$ is the configurational factor which depends upon the physical model and the assumptions underlying the derivation of the isotherm, θ is the degree of surface coverage, C is the concentration of the inhibitor in the bulk electrolyte, x is the size factor ratio, 'a' is the molecular interaction parameter and 'b' is the equilibrium constant of the adsorption process. In this study, adsorption of *FB* gum was found to agree with the Frumkin adsorption model Eq. (8);

$$\log\left(\frac{\theta}{1-\theta}\right)[C] = \log b + 2a\theta \quad (8)$$

where θ is the degree of surface coverage, C is the concentration of the adsorbate, b is the adsorption coefficient which represents the adsorption-desorption equilibrium constant and 'a' is the interaction parameter. From Eq. (8), a plot of $\log\left(\frac{\theta}{1-\theta}\right)[C]$ versus θ should be linear if Frumkin isotherm is obeyed.

Figure 7 shows the Frumkin isotherm for the adsorption of *FB* gum on the surface of aluminum. Adsorption parameters deduced from the plots revealed that the adsorption of *FB* gum on Al surface fitted the Frumkin model excellently ($R^2 = 0.9967$ and 0.9381 at 303 and 333 K, respectively). The results also revealed that the interaction parameter ($a = 2.8$ and 3.8 at 303 and 333 K) are positive and increases with temperature, hence there is attraction between the adsorbed inhibitor's molecules and the extent of attraction increases with an increase in temperature.

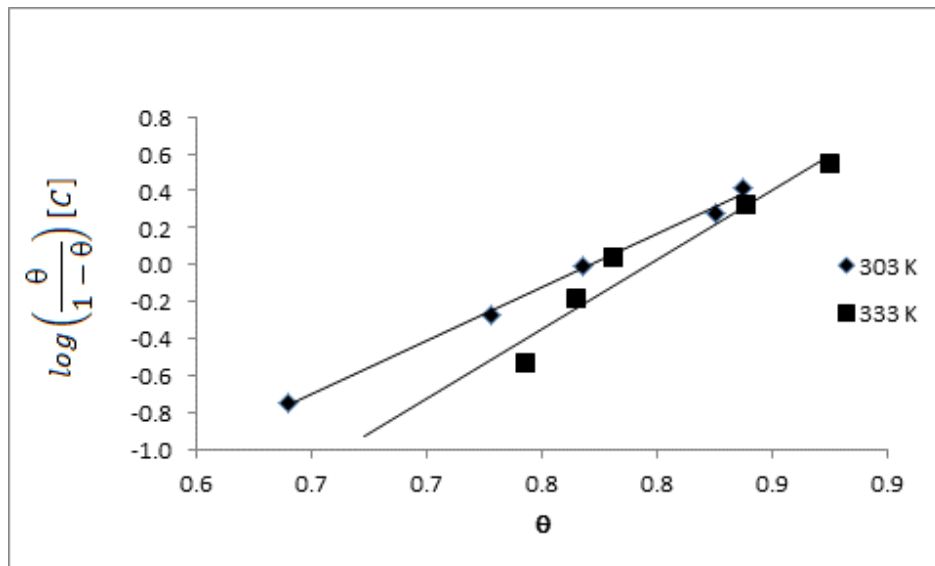


Figure 7 Frumkin isotherm for the adsorption of *FB* gum on Al surface.

Table 6 Activation energy and heat of adsorption of various concentrations of *FB* gum on an Al surface.

C (g/L)	E _a (kJ/mol)	Q _{ads} (kJ/mol)
Blank	75.74	-
0.1	66.26	53.70
0.2	71.49	27.96
0.3	74.11	12.36
0.4	77.96	23.68
0.5	82.94	89.35

The equilibrium constant of adsorption, ‘*b*’ derived from the Frumkin model is related to the standard free energy of adsorption according to Eq. (9) [23];

$$b = \frac{1}{55.55} \exp\left(\frac{\Delta G_{ads}^0}{RT}\right) \tag{9}$$

where ΔG_{ads}^0 is the standard free energy of adsorption of *FB* gum on an Al surface, 55.55 is the molar concentration of water in the acid solution, R is the gas constant and T is the absolute temperature. In this study, calculated values of ΔG_{ads}^0 were -35.10 and -45.15 kJ/mol at 303 and 333 K, respectively. Although the free energy value at 303 K is slightly less than the threshold value (-40 kJ/mol), the calculated free energies nevertheless fail to support the mechanism of electron transfer from the inhibitor to a vacant d-orbital in the metal surface. The data also suggest that at lower temperature, the mechanism of physical adsorption was apparent while chemisorption dominated at higher temperatures.

In order to confirm the mechanism of adsorption of *FB* gum on the surface of Al, the experimental data was also fitted into the Dubinin-Radushkevich isotherm model (D-RIM), expressed in Eq. (10) [24].

$$\ln(\theta) = \ln(\theta_{max}) + a\delta^2 \tag{10}$$

where θ_{max} is the maximum surface coverage and δ (Polany potential) can be correlated as;

$$\delta = RT \ln\left(1 + \frac{1}{C}\right) \tag{11}$$

The constant, ‘*a*’ gives the mean adsorption energy, E_{ads} , i.e. $E_{ads} = 1/(2a)^{0.5}$, R is the gas constant and T is the absolute temperature. The transfer energy (E_{ads}) of 1 mol of adsorbate from infinity (bulk solution) to the surface of the adsorbent is an index for predicting the mechanism of adsorption of the inhibitor. When E_{ads} is less than 8 kJ/mol, a physical adsorption mechanism is upheld and vice versa. **Figure 8** shows the D-RIM isotherms for the adsorption of *FB* gum on the surface of Al. The fitness of the data was excellent ($R^2 = 0.9616$ and 0.8555 at 303 and 333 K, respectively) and calculated values of E_{ads} were 10.00 and 10.50 kJ/mol at 303 and 333 K, respectively. This supports the mechanism of chemical adsorption as proposed earlier. Values of θ_{max} were calculated as 0.9148 and 0.9308 at 303 and 333 K, respectively, indicating that the maximum theoretical coverage for *FB* gum onto the Al surface at 303 and 333 K, respectively, corresponded to inhibition efficiencies of 91.48 and 93.08 %, respectively. The observed theoretical trend (i.e. increase in inhibition efficiency with temperature) shows slight deviation from the maximum inhibition efficiencies obtained from the experiment suggesting that these values may be attainable at higher concentrations (i.e. $C > 0.5$ g/L of *FB* gum) and not within the range of concentrations used in the present study. Nevertheless, the observed trend also supports the mechanism of chemical adsorption.

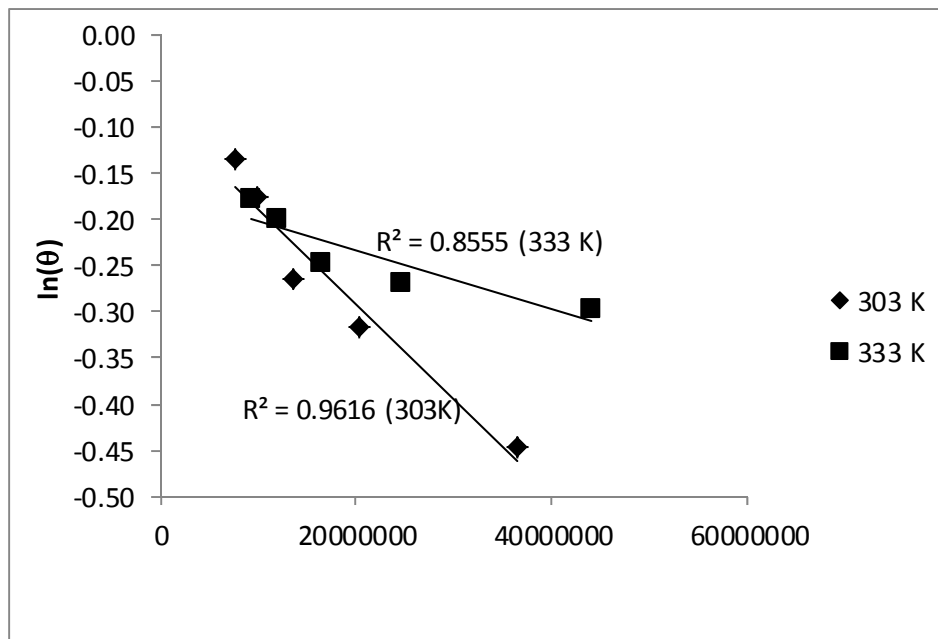
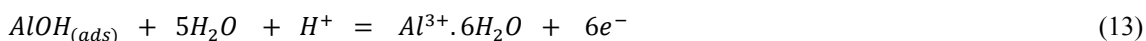


Figure 8 D-RIM isotherms for the adsorption of *FB* gum on the surface of Al.

Mechanism of inhibition

The corrosion of Al in aqueous solution is a function of the concentration of anions in the system. HCl is a strong acid and can ionize to produce a chloride ion, which can attack the Al metal. The mechanism for the inhibition of the corrosion of aluminum in solution of HCl is similar to that proposed by Ford *et al.* [25], Nguyen and Foley [26] and are presented in Eqs. (12) - (15);



The controlling step in the metal dissolution is the complexation reaction between the hydrated cation and the anion (Eq. (15)), which is feasible in the presence of chloride ions generated by ionization of HCl. Adsorption of the inhibitor on the surface of the metal will reduce the surface area available for anodic and cathodic reactions. According to Khaled [27], organic molecules inhibit corrosion by adsorption at the metal/solution interface and the adsorption depends on the molecule’s chemical composition, the temperature and the electrochemical potential at the metal/solution interface. In the case of the aluminum surface, the solvent H₂O molecules could also adsorb on the aluminum oxide surface forming hydroxylated sites, or hydroxide layers at the surface (Eqs. (14) and (15)), that impart a pH-dependent surface charge. The polar hydroxyl groups may cause the surface to attract and physically adsorb a single or several additional layers of polar water molecules. In acidic solution, the positively charged surface sites will electrostatically attract any anions present in solution, and repel cations. *FB* gum may be adsorbed on the aluminum oxide surface in four different ways [27];

- i. Electrostatic interactions between a negatively charged surface, which is provided by the adsorbed chloride ion and the positively charged/protonated inhibitor.
- ii. Interaction of unshared electron pairs in the inhibitor's molecule with the aluminum surface,
- iii. Interaction of π -electron(s) with the aluminum surface.
- iv. A combination of the (i-iii) types.

Efficient adsorption is the one that arises from an interaction between the π -electron(s) or hetero atom(s) in the *FB* gum molecule. Chemical adsorption seems to be the most important type of interaction between the Al_2O_3 surface and *FB* molecules. Here, the adsorbed species are in contact with the Al_2O_3 surface. In this process, a coordinated bond that involves electron transfer from the inhibitor system towards the metallic surface is formed. The electron-transfer may be facilitated by a lone pair of electrons in the inhibitor and the availability of π -electrons due to the presence of double bonds or aromatic rings in its structure. Moreover, there is a great possibility that adsorption may also take place via hydrogen bond formation between the X-H linkage (X may be hetero atom) in some of the constituents of *FB* gum and the oxygen atoms of the aluminum oxide/aluminum hydroxide surface species. This type of adsorption should be more prevalent for protonated X-atom(s), because the positive charge on the X-atom may be conducive to the formation of hydrogen bonds. Unprotonated X-atoms may also be adsorbed by direct chemisorption, as mentioned previously, or by hydrogen bonding to a surface oxidized species. The extent of adsorption by the respective modes depends on the nature of the metal surface. A good inhibitor must have strong affinity for the bare metal atoms. The requirement is different in case of aluminum; a compact passive oxide film is always present on the electrode surface, where hydrogen bond formation accounts for most of the inhibition action. An effective inhibitor is one that forms hydrogen bonds easily with the oxidized surface.

Conclusions

From the experimental results obtained in the present study, the following conclusions can be drawn

- 1) *FB* gum is yellowish odourless, mild acidic and ionic.
- 2) The chemical constituents of *FB* include albiotic acid (1.00 %), hexadecanoic acid (4.41 %), 9-octadecanoic acid (1.00 %), stearic acid (3.01 %), oleic acid (0.10 %), octadecanoic acid (9.12 %), 6,13-pentacenequinone (20.43 %), d-glucose (18.69 %) and sucrose (42.23 %).
- 3) *FB* has been found to be a good adsorption inhibitor. Its inhibition proceeded via the mechanism of physical adsorption (the reasons are inhibition efficiency decreases with increasing temperature E_a and ΔG_{ads}^0 values were lower than threshold values of 80 and -40 KJ/mol and was best described by a Langmuir adsorption model).
- 4) Inhibition of mild steel by *FB* gum occurred through synergistic adsorption of the various components of the gums hence the formation of multiple adsorption layers is proposed.

References

- [1] P Arora, S Kumar, MK Sharma and SP Mathur. Corrosion inhibition of aluminium by *Capparis deciduas* in acidic media. *E-J. Chem.* 2007; **4**, 450-6.
- [2] Z Ghasemi and A Tizpar. The inhibition effect of some amino acids towards Pb-Sb Se As alloy corrosion in sulfuric acid solution. *Appl. Surf. Sci.* 2006; **252**, 3667-72.
- [3] SB Elayyoubi, S Hammouti, HO Kertit and EB Maarouf. Corrosion inhibition of mild steel in hydrochloric acid solutions by malonitrile compounds. *Rev. Met. Paris* 2004; **2**, 153-7.
- [4] BEA Rani and BB Basu. Green inhibitors for corrosion protection of metals and alloys: An overview. *Int. J. Corros.* 2012; **2012**, 380217.
- [5] BI Ita. 4-Formylmorpholine hydrazone and 4-formymorpholine: New corrosion inhibitors for mild steel in 0.1 M in hydrochloric acid solution. *In: Proceedings of the Chemical Society of Nigeria, Nigeria*, 2004, p. 10-21.

- [6] BI Ita. A study of corrosion inhibition of mild steel in 0.1M hydrochloric acid by O-Vanilin hydrazone. *Bull. Electrochem.* 2004; **20**, 363-70.
- [7] BI Ita. Inhibition of mild steel corrosion in hydrochloric acid by anisaldehyde and anisaldehyde glycine. *Bull. Electrochem.* 2005; **21**, 219-323.
- [8] BI Ita and OE Offiong. The inhibition of mild steel corrosion in hydrochloric acid by 2,2'-pyridil and ∞ -pyridon. *Mater. Chem. Phys.* 1997; **51**, 203-10.
- [9] J Fang and J Li. Quantum chemistry study on the relationship between molecular structure and corrosion inhibition efficiency of amides. *J. Mol. Struct.* 2002; **593**, 179-85.
- [10] NO Eddy, FE Awe, AA Siaka, L Magaji and EE Ebenso. Chemical information from GC-MS studies of ethanol extract of *Andrographis Paniculata* and their corrosion inhibition potentials on mild steel in HCl solution. *Int. J. Electrochem. Sci.* 2011; **6**, 4316-28.
- [11] SA Umoren and EE Ebenso. Studies of anti-corrosive effect of *Raphia hookeri* exudates gum-halide mixtures for aluminium corrosion in acidic medium. *Pigment Resin Tech.* 2008; **37**, 173-82.
- [12] J Buchweishaija and GS Mhinzi. Natural products as a source of environmentally friendly corrosion inhibitors: The case of gum exudate from *Acacia seyal var.* *Electrochim. Acta.* 2008; **26**, 257-65.
- [13] EE Oguzie, CK Enenebeaku, CO Akalezi, SC Okoro, AA Ayuk and EN Ejike. Adsorption and corrosion-inhibiting effect of *Dacryodis edulis* extract on low-carbon-steel corrosion in acidic media. *J. Colloid Interf. Sci.* 2010; **349**, 283-92.
- [14] PO Ameh. Adsorption and inhibitive properties of *Khaya ivorensis* gum for the corrosion of mild steel in HCl. *Int. J. Modern Chem.* 2012; **2**, 28-40.
- [15] NO Eddy, AO Odiongenyi, PO Ameh and EE Ebenso. Corrosion inhibition potential of *Daniella oliverri* gum exudate for mild steel in acidic medium. *Int. J. Electrochem. Sci.* 2012; **7**, 7425- 39.
- [16] M Abdallah. Guar gum as corrosion inhibitor for carbon steel in sulphuric acid solutions. *Port. Electrochim. Acta* 2004; **22**, 161-75.
- [17] PO Ameh and NO Eddy. *Commiphora pedunculata* gum as a green inhibitor for the corrosion of aluminium alloy in 0.1 M HCl. *Res. Chem. Intermed.* 2014; **40**, 2641-9.
- [18] M Behpour, SM Ghoreishi, M Khayatkashani and N Soltani. The effect of two oleo-gum resin exudate from *Ferula assa-foetida* and *Dorema ammoniacum* on mild steel corrosion in acidic media. *Corros. Sci.* 2011; **53**, 2489-501.
- [19] NO Eddy, PO Ameh, MY Gwarzo, IJ Okop and SN Dodo. Physicochemical study and corrosion inhibition potential of *Ficus tricopoda* for aluminium in acidic medium. *Port. Electrochim. Acta* 2013; **31**, 79-93.
- [20] SJ Carter. *Tutorial Pharmacy: Solution.* Great Britain, Pitman Press, 2005, p. 1-8.
- [21] NO Eddy, SE Abechi, PO Ameh and EE Ebenso. GCMS, FTIR, SEM, physiochemical and rheological studies on *Albizia zygia* gum. *Walailak J. Sci. & Tech.* 2013; **10**, 247-65.
- [22] A Chetounani, B Hammouti and M Benkaddour. Corrosion inhibition of iron in hydrochloric acid solution by jojoba oil. *Pigment Resin Tech.* 2004; **33**, 26-31.
- [23] NO Eddy. Ethanol extract of *Phyllanthus Amarus* as a green inhibitor for the corrosion of mild steel in H₂SO₄. *Port. Electrochim. Acta* 2009; **27**, 579-89.
- [24] AA Khadam, AS Yaro, AY Musa, AB Mohamad and AAH Kadhum. Corrosion inhibition of copper-nickel alloy: Experimental and theoretical studies. *J. Korean Chem. Soc.* 2012; **56**, 406-15.
- [25] FP Ford, GT Burstein and TP Hoar. Bare surface reaction rates and their relation to environment controlled cracking of aluminum alloys. *J. Electrochem. Soc.* 1980; **127**, 1325-31.
- [26] H Nguyen and RT Foley. Chemical nature of aluminum corrosion. *J. Electrochem. Soc.* 1982; **129**, 464-7.
- [27] KF Khaled. Electrochemical investigation and modeling of corrosion inhibition of aluminum in molar nitric acid using some sulphur-containing amines. *Corros. Sci.* 2010; **52**, 2905-16.